

DETC03/DAC-0000

TOPOLOGY AND SHAPE OPTIMIZATION OF AN INTERBODY FUSION IMPLANT FOR LUMBAR SPINE FIXATION

Andrés Tovar*, John E. Renaud†, James J. Mason‡, Shawn E. Gano*

Department of Aerospace and Mechanical Engineering
University of Notre Dame
Notre Dame, Indiana 46556
Email: jrenaud@nd.edu

ABSTRACT

The goal of this research is to obtain the optimum design of a new interbody fusion implant for use in lumbar spine fixation. A new minimally invasive surgical technique for interbody fusion is currently in development. The procedure makes use of an interbody implant that is inserted between two vertebral bodies. The implant is packed with bone graft material that fuses the motion segment. The implant must be capable of retaining bone graft and supporting spinal mechanical loads while fusion occurs. Finite element-based optimization techniques are used to drive the design. The optimization process is performed in two stages: topology optimization and shape optimization. Four independent load conditions are analyzed: compression, flexion, extension, and lateral bending. The resulting optimal geometries for each load condition are superimposed to generate an optimum design that is converted to a candidate implant geometry suitable for manufacturing.

NOMENCLATURE

x_e	Design variable.
ρ_0	Original density of the material.
E_0	Original Young's modulus of the material.
ρ_e	Density of the element.
E_e	Young's modulus of the element.
e	Element number subscript.

N	Number of (finite) elements.
p	Penalization power.
F_G	Global node force vector.
U_G	Global node displacement vector.
K_G	Global stiffness matrix.
V	Total potential energy.
U	Internal potential energy.
Ω	External potential energy.
u_e	Element node displacement.
k_e	Element stiffness matrix.
M	Total mass.
f	Objective function.
x_{min}	Lower limit for the design variable.
x_{max}	Upper limit for the design variable.
k_0	Original element stiffness matrix of the material.
q	Ratio between E_{min} and E_0 .
E_{min}	Minimum value allowed for Young's modulus.
$\hat{\sigma}$	Von Mises stress.
S_f	Fatigue stress.

INTRODUCTION

Lower back pain is one of the most common and significant musculoskeletal problems in the world. It has been estimated that 80% of Americans will experience lower back pain in their lifetime. Currently there are 600,000 surgeries performed per year in USA, with a 50% of failure rate. This high failure rate has motivated the development of new surgical procedures that

*Graduate Research Assistant.

†Professor, ASME Fellow

‡Associate Professor, ASME Member

are less invasive and more successful. One of the leading causes of lower back pain is related to disc disorders. Spinal discs are located between each vertebra in the spine and are designed to act as shock absorbers within the spine. In some cases, with time, they deteriorate and lose their shock absorbing capabilities causing pain in the spine and/or vertebra. Figure 1 depicts some disc disorders that can occur in the spine.

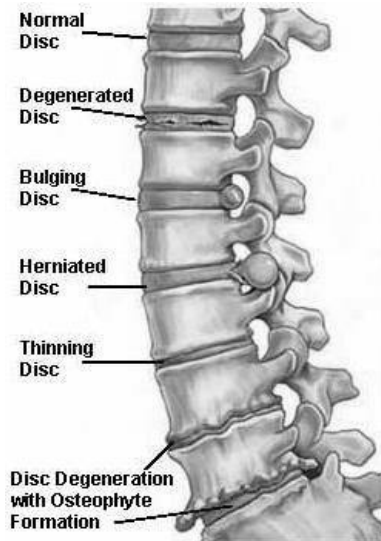


Figure 1. DISC DISORDERS

For many disc disorders it is difficult to treat them through non-surgical methods. The most common surgical practice to alleviate the pain associated with these disorders is lumbar fusion. The objective of this technique is to eliminate the relative movement across a motion segment of the spine, or a series of motion segments, that have degenerated to the point of causing pain.

Lumbar spinal fusion involves the use of bone graft material and fixation instrumentation to prevent motion in the painful vertebral segment. The bone graft grows between the two vertebral bodies and fuses the motion segment. Spine surgery instrumentation like plates, rods and cages are used to provide fixation as part of the fusion surgery process. There are several types of spinal fusion surgery options described in literature [1]. The research presented in this investigation relates to a new surgical procedure for lumbar spine fixation that is currently in development. The new minimally invasive surgical procedure involves the use of a novel interbody fusion implant. The function of this implant is to house the bone graft material while insuring structural stability of the motion segment, while the bone graft heals. The healing process can take several months.

Our goal in this work is to obtain the optimal geometry of

the interbody fusion implant. One wants to maximize the volume available for bone graft material within the implant, while supporting the structural loads imposed on the system. The optimization process is performed in two stages. The first stage seeks to minimize strain energy under mass fraction constraints using a topology optimization technique. The second stage seeks to minimize mass under stress constraints using a shape optimization technique. GENESIS, a finite element-based optimization software, is used to drive the optimum design. Increasingly, topology optimization is being used to find preliminary, sometimes completely innovative, structural configurations that meets specific conditions (i.e. objective function and constraints). Shape optimization is used to tune the preliminary design using a more defined geometry. The automotive industry regularly uses topology and shape optimization software tools for the design of innovative structures.

FINITE ELEMENT-BASED OPTIMIZATION

Finite element-based optimization techniques were first developed by UCLA Professor, Lucien Schmit in the 1960s. He recognized the potential of combining optimization techniques with finite element analysis for structural design. Today, three types of finite element-based optimization approaches are often available within commercial FEA software: sizing, shape and topology optimization. These approaches for structural optimization are differentiated by the use of different design variable types.

Sizing optimization

Sizing or parameter optimization typically uses element cross-sectional properties as design variables [2]. These include parameters such as plate thickness, area and moment of inertia of a beam cross section.

Shape optimization

Shape optimization involves determining the optimal profile (i.e. boundary) of a structural component. In this technique the grid is perturbed in order to find its optimum shape. The design variables are related to the amount of deformation. Approaches to shape optimization include: basis vector and grid perturbation approach.

Basis vector approach This approach requires the definition of several trial designs call basis vectors. The design variables are the weight parameters that define the participation of each basis vector in the design process.

Grid perturbation approach This approach requires the definition of vectors to define the direction of a perturbation

in the grid. The design variables are the values that determine the amount of the perturbation in the design process.

Basis and perturbation vectors can be automatically generated in programs like GENESIS [3]. The technical challenge associated with this approach is the mesh parameterization. Specifically, how do we relate the displacement of the grid during the perturbation. Figure 2 depicts a perturbation over a square grid, and illustrates how the mesh is parameterized to create a new smooth grid.

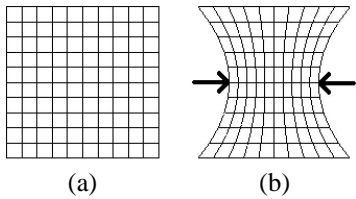


Figure 2. (a) ORIGINAL GRID (b) PERTURBED GRID

Topology optimization

Topology optimization involves the optimal distribution of material within a structure. Unlike shape and sizing optimization, topology optimization does not require an initial design. Typically, the design process starts with a block of material called the design domain. The design domain is comprised of a large number of candidate elements, and the topology optimization process selectively removes from the domain those unnecessary elements. The design variables in topology optimization depend on the type of material model used in the finite element analysis. There are two general approaches: density and homogenization.

Density approach In the density approach, presented by Bendsøe [4], the design variables x_e are the element relative densities or volume fraction (fraction of solid material). The material model, for each finite element, is based on heuristic relationships between design variables and material properties (i.e. density and Young’s modulus). Simple relationships that have been used, are

$$\rho_e = x_e \rho_0 \tag{1}$$

$$E_e = (x_e)^p E_0, \tag{2}$$

where x_e is the design variable, ρ_0 and E_0 are the original density and Young’s modulus of the material, ρ_e and E_e are the density and Young’s modulus of the element, subscript e is the element number, and p is the penalization power where $p \geq 1$. This material model leads to an isotropic material [5]. In theory Eqns.

(1) and (2) are true only if the design variables are 0.0 or 1.0. If $x_e = 1.0$ then the element is needed, if $x_e = 0.0$ then the element can be removed from the model [6].

Homogenization approach In the homogenization approach, presented by Bendsøe and Kikuchi [7], each element is a microstructure. The design variables are the parameters of the microstructure. In two dimensions, the microstructure consists of millions of unit square cells oriented at an angle α . Each cell has a rectangular hole defined by side lengths a and b . The design variables correspond to the three parameters: a , b and α . These parameters are illustrated in Fig. 3. In this approach the model leads to a more general orthotropic material.

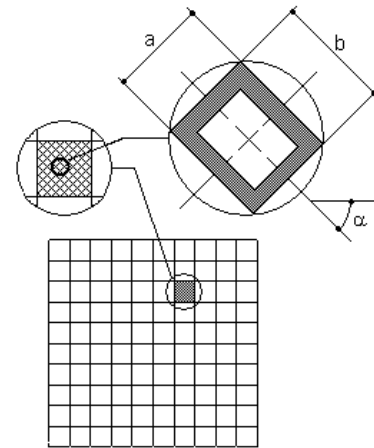


Figure 3. HOMOGENIZATION APPROACH

The code, Optistruct, originally developed by Kikuchi et al., and now being enhanced by Altair Computing, uses the homogenization approach [8]. The software GENESIS, from VR&D, uses the density approach [6].

TOPOLOGY OPTIMIZATION

The first stage in the optimum design of the interbody fusion implant is to perform a topology optimization over the design domain. The idea is to obtain a first approximation of the optimum geometry, to be tuned using shape optimization.

Optimization problem

The topology optimization problem is developed through an elasticity analysis of the finite element model. Using linear elas-

ticity and the principle of virtual work, we have,

$$F_G = K_G U_G, \quad (3)$$

where U_G and F_G are the global node displacement and force vectors, K_G is the global stiffness matrix. The total potential energy is given by

$$V = U + \Omega, \quad (4)$$

where U and Ω are the internal and external potential energies respectively [9]. The internal or strain energy for N (finite) elements is

$$U = \frac{1}{2} \sum_{e=1}^N u_e^T k_e u_e, \quad (5)$$

where u_e is the element node displacement vector and k_e is the element stiffness matrix. Now, the total mass M is the sum of the elemental masses ρ_e defined by Eqn. (1), this is

$$M = \sum_{e=1}^N \rho_e. \quad (6)$$

The design task is formulated as a topology optimization problem where the objective function seeks to minimize both strain energy U and mass M defined by Eqns. (5) and (1). The optimization problem can be stated as

$$\left. \begin{array}{l} \min f = \sum_{j=1}^3 U^{(c)} + M \\ \text{s.t. } K_G U_G = F_G \\ x_{min} \leq x_e \leq 1.0 \end{array} \right\}, \quad (7)$$

where f is the multiobjective function, x_{min} is the lower limit for the design variables, and $e = 1, \dots, N$. The subindex $c = 1, 2, 3$ represents the load case: flexion/extension, lateral bending and compression. Normally different weight values will be imposed on the terms of a multiobjective function. Since topology optimization is meant to give an approximation of the final design, the weight values are taken equal to one. Each term in the multiobjective function is normalized such that the initial value of each one is equal to one. Then the initial condition corresponds to $f = 4$.

Using the density approach given by Eqns. (1) and (2), the optimization problem can be expressed in terms of the design

variables x_e . In particular, the element stiffness matrix k_e can be written as,

$$k_e = (x_e)^p k_0, \quad (8)$$

where k_0 is the original element stiffness matrix of the material. The penalization power is typically $p = 3$. This approach, used by Sigmund [10], requires a non-zero design variable to avoid singularity conditions, typically $x_{min} = 0.001$. The software GENESIS has implemented several different relationship functions between design variables and material properties [6]. By default it uses Eqn. (1), but instead of Eqn. (8) it uses

$$k_e = q k_0 + (1 - q)(x_e)^p k_0, \quad (9)$$

where the penalization power is typically $2.0 \leq p \leq 3.0$. We define the parameter $q = \frac{E_{min}}{E_0}$, where E_{min} is the minimum value that Young's modulus is allowed to take, where $0.0 < q \leq 1.0$, gives a typical value of $q = 10^{-6}$. There are several approaches to solve the structural optimization problem given by Eqn. (7). Some of the most common techniques include: Approximation concepts for structural optimization [11], Optimality Criteria (OC) [12], Sequential Linear Programming (SLP), and Method of Moving Asymptotes (MMA) [13]. GENESIS has incorporated approximation techniques [6].

Finite Element Model

The finite element analysis and topology optimization software GENESIS is used to drive the topology design of the interbody fusion implant. The implant will be inserted within the annulus fibrosus of the disc after removal of the nucleus pulposus (i.e., percutaneous nucleotomy). Figure 4 provides a conceptual illustration of the implant within the disc in a cross-sectional (transverse) view.

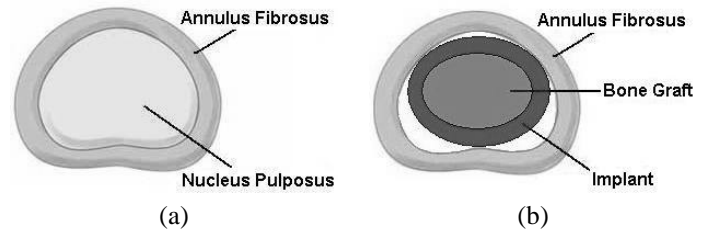


Figure 4. INTERVERTEBRAL DISC (a) NORMAL (b) IMPLANTED

The design domain for topology optimization is constrained by the geometry of the annulus fibrosus. The maximum lengths

for the design domain define a volume of 40 mm length, 30 mm width and 8 mm height. In this study, as Fig. 5 depicts a symmetric design domain composed of 8256 eight-noded solid CHEXA elements and 9928 grid nodes is used. The mechanical properties: Young's modulus E_0 , density ρ_0 and Poisson's ratio ν , correspond to that of the polymethyl methacrylate (PMMA) bone cement.

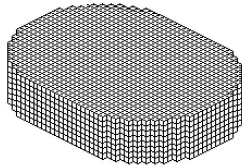


Figure 5. DESIGN DOMAIN

The vertebral bodies above and below the implant, are considered rigid elements. The lower vertebra is modeled by fully constraining the bottom of the design space. The upper vertebra is modeled by one rigid element RBE2 that spans the compressive half of the implant. The independent node, that controls the motion of the rigid element, is located in the center at the top surface of the upper vertebra. The dependent nodes are on the upper surface of the implant. Figure 6 illustrates the shape and the relative (rotational) motion of the rigid elements (vertebral bodies L4-L5).

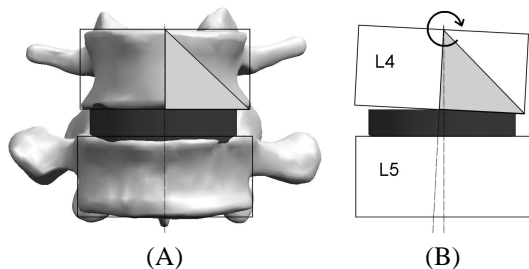


Figure 6. MOTION SEGMENT (A) NATURAL POSITION (B) ROTATED

Normal load conditions for an intervertebral lumbar disc, which are most often reported in literature, [14] [15], [16], are 400 N for the compressive load, and 7.5 Nm for the moment loads. These moments are applied in the center of the upper vertebra located 25 mm above the upper surface of the design domain.

Figure 7 shows the three load conditions used for The topology optimization: flexion/extension (M_x), lateral bending (M_y), and compression (F_z). Symmetry conditions are imposed for the

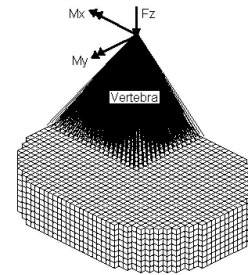


Figure 7. LOAD CONDITIONS

model. The final topology of the implant must provide maximum volume for the bone graft material to grow into the vertebral bodies. Previous implant designs show that this space corresponds to a mass fraction not higher than 50%, and usually around 35%.

Results

The topology optimization problem is solved for three loading conditions: compression, flexion/extension, and lateral bending using Eqn. (7). The optimum solution is found in fifteen iterations as shown in Fig. 8.

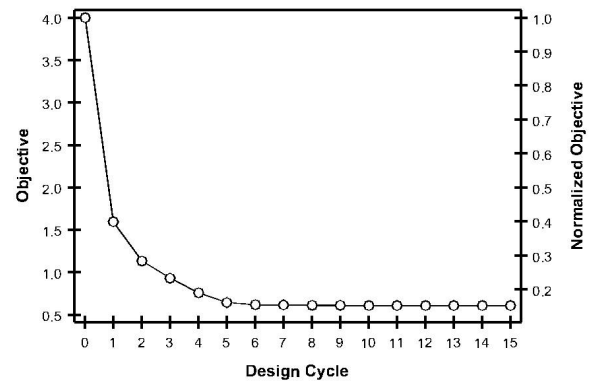


Figure 8. OBJECTIVE FUNCTION EVALUATION

Figure 9 shows the optimum shape for the load conditions applied. This solution is used to obtain the final topology applying symmetry conditions.

Analysis

To illustrate the benefit of applying topology optimization for the design of the interbody fusion implant, the results obtained in this study are compared to candidate designs generated using a trial and error approach for geometry design. A finite element analysis of the best implant generated by trial and error is compared to the new candidate implant proposed from the

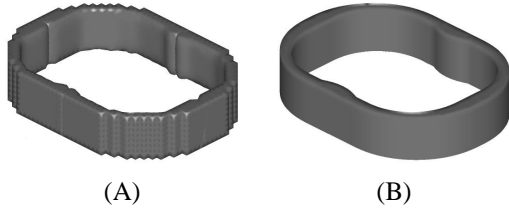


Figure 9. TOPOLOGIES (A) INITIAL (B) TUNED

topology optimization studies. The combined loading conditions of the finite element analysis are the compressive load (400 N), the flexion/extension moment (7.5 Nm), and the lateral bending moment (7.5 Nm). The vertebra is modeled as a rigid element. The lower surface of the implant is completely constrained. Table 1 compares the values of the finite element analysis for the optimal implant topology to that of the previous best design using relative values listed as a percentage. The analysis includes maximum nodal displacement and maximum von Mises stress. We observe a significant decrease (i.e., improvement) in all three metrics of performance. The maximum von-Mises stress, nodal strain energy and nodal displacement are significantly lower for the optimum topology.

Table 1. TOPOLOGY OPTIMIZED IMPLANT ANALYSIS AND PERCENTAGE VALUES RELATIVE TO THE TRIAL AND ERROR IMPLANT

	Displ [m]		S Energy [Pa]		vM Stress [Pa]	
Compr	3.5e-6	87%	0.3e3	75%	1.84e6	92%
Flexion	20.1e-6	44%	24.0e3	85%	11.4e6	35%
Extension	20.1e-6	79%	24.0e3	75%	11.4e6	26%
L. Bend	16.4e-6	67%	9.75e3	42%	7.2e6	73%

SHAPE OPTIMIZATION

An initial geometry of the optimum structure has been defined in topology optimization. The geometric features were set in order to obtain a model to be optimized in a more detailed scale. Once the geometry is defined for the new implant, we can apply the shape optimization strategy.

Optimization problem

The final design task is formulated as a shape optimization problem where the objective function is to minimize mass M con-

strained by a maximum elemental von Mises stress $\hat{\sigma}$,

$$\left. \begin{array}{l} \min : M \\ \text{s.t.} : \hat{\sigma}^{(c)} < S_f \\ K_G U_G = F_G \\ x_{min} \leq x_e \leq x_{max} \end{array} \right\}, \quad (10)$$

where the superindex $c = 1, 2, 3$ represents the load case: flexion/extension, lateral bending and compression, and S_f is a fatigue stress. According to data published by Lewis related to bone cement properties [17], an amplitude of uniaxial compressive load $S_f = 7.5$ MPa, allows for a minimum of 65,970 to a possible more than 1.5 million of stress cycles. Then this value will be used to constrain the maximum von Mises stress in the shape optimization problem.

To perform shape optimization, the grid perturbation approach is used in this work. The perturbation vectors are applied on the limit of specific set of nodes (i.e. domain). The deformation of the grid in the domains, defines the final shape of the implant. Figure 10 illustrates the domains and the perturbation vectors corresponding to a quarter of the implant. Symmetry conditions are imposed on this model.

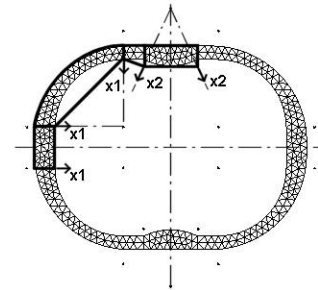


Figure 10. DOMAINS AND PERTURBATION VECTORS

The design variables x_1 and x_2 , correspond to the magnitudes of perturbation vectors. They control the thicknesses of the implant. Appropriate domains are related with the design variables in order to maintain the geometric relations of the inner boundary of the implant. The initial value defined for the magnitude of x_1 and x_2 is set equal to zero. Their upper and lower limits x_{max} and x_{min} are chosen as big as the geometry allows.

Finite Element Model

In order to determine final dimensions of the implant, a more detailed finite model is obtained. This is new model is composed by 6751 six-noded solid CPENTA elements and 4585 nodes. Once again, the vertebra was modeled as a rigid element acting

in compression. Symmetric boundary conditions are imposed to the model. Figure 11 depicts the new layout.

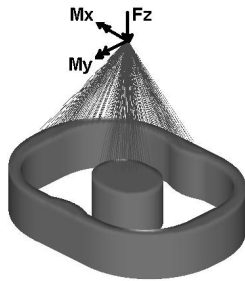


Figure 11. FINITE ELEMENT MODEL

Results

The shape optimization problem is solved for the three load conditions and the two defined design variables. The initial condition of the model is infeasible since the maximum von Mises stress $\hat{\sigma}$ is greater than the imposed constrain $S_f = 7.5$ MPa. After six iterations the optimum values for the design variables are $x_1 = 1.650$ mm, and $x_2 = 1.516$ mm. Figure 12 shows the objective values of the objective function and the constraint violation along the shape optimization process.

Analysis

As a result of the shape optimization, the mass of the implant increased 14% respect to the initial design (from the topology optimization). The addition of material is to avoid the risk of fatigue failure in the implant. The final analysis is performed using the normal values for loading: compressive load (400 N), flexion/extension moment (7.5 Nm), and the lateral bending moment (7.5 Nm).

The vertebra is modeled as a rigid element. The lower surface of the implant is completely constrained. Figure 13 the mass and the von Mises stress for the load conditions. We observe a significant improvement from the first trial and error design, to the shape optimized one.

SUMMARY AND CONCLUSIONS

A candidate geometry for an interbody fusion implant is obtained using topology and shape optimization methods. The topology optimization seeks to minimize strain and mass fraction. This initial structure is fine tuned using a shape optimization technique. This technique seeks to minimize mass constrained by a maximum von Mises stress. The implant is subject to three different loading cases. These load cases are analyzed

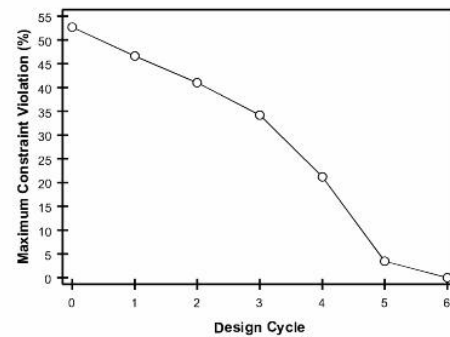
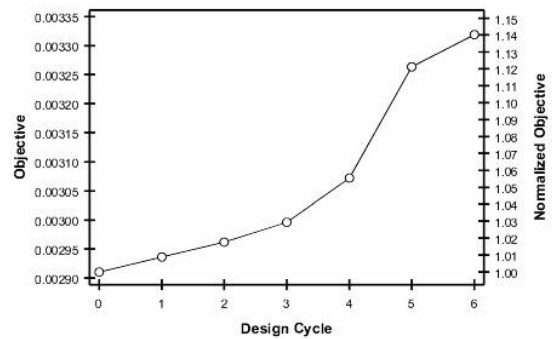


Figure 12. OBJECTIVE FUNCTION AND CONSTRAINT VIOLATION EVALUATION

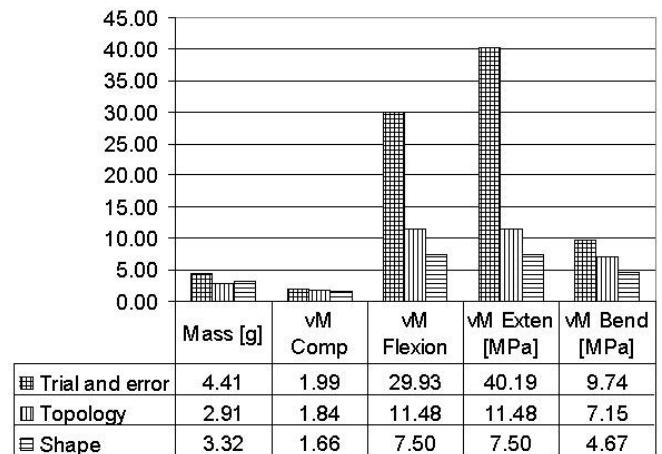


Figure 13. COMPARATIVE RESULTS

along the optimization process. The implant is designed to restrain bone graft material while maintaining proper intervertebral spacing during spinal fusion. In comparison to previous implant design studies using finite element analysis, the new candidate geometry provides better structural stability for the load condi-

tions of compression, flexion/extension and lateral bending.

ACKNOWLEDGMENT

Support for this research has been provided by: Universidad Nacional de Colombia, Colombian Institute for Development of Science and Technology "Francisco Jose de Caldas" - COL-CIENCIAS, the Fulbright Program, NSF Grant DMI01-14975, and the State of Indiana 21st Century Research and Technology Fund.

REFERENCES

- [1] White, A. H., Rothman, R. H., and Ray, C. D., Eds., 1987. *Lumbar spine surgery*. The C. V. Mosby Company.
- [2] Leiva, J. P., Watson, B. C., Kosaka, I., and Vanderplaats, G. N., 2002. "Dynamic finite element analysis and optimization in genesis". In Proceedings of the 9th AIAA/ISSMO Symposium on Multidisciplinary Analysis and Optimization.
- [3] Leiva, J. P., and Watson, B. C., 1999. "Shape optimization in the genesis program". In Proceedings of Optimization in Industry II.
- [4] Bendsøe, M. P., 1989. "Optimal shape design as a material distribution problem". *Struct. Optim.*, **1** [], pp. 193–200.
- [5] Belegundu, A., and Chdrupatla, T., 1999. *Optimization Concepts and Applications in Engineering*. Prentice Hall.
- [6] , 2001. *GENESIS User's Manual, Version 7.0*, vol. I: Overview. VR & R, Colorado Springs, CO, August, pp. 299–303.
- [7] Bendsøe, M. P., and Kikuchi, N., 1988. "Generating optimal topologies in optimal design using a homogenization methods". *Comp. Meth. Appl. Mech. Engrg*, **17** [], pp. 197–224.
- [8] Leiva, J. P., Watson, B. C., and Kosaka, I., 1999. "Modern structural optimization concepts applied to topology optimization". In Proceedings of the 40th AIAA/ASME/ASCE/AHS/ASC Structures, Structural Dynamics, and Material Conference, pp. 1589–1596.
- [9] Bickford, W. B., 1990. *A First Course in the Finite Element Method*. Richard D. Irwin, Inc.
- [10] Sigmund, O., 2001. "A 99 line topology optimization code written in matlab". *Struct. Multidisc. Optim.*, **21** [], pp. 120–127.
- [11] Schmit, L. A., 1974. "Some approximation concepts for structural synthesis". *AIAA J.*, **12** [], pp. 692–699.
- [12] Bendsøe, M. P., 1995. *Evolutionary structural optimization*. Springer, New York.
- [13] Svanberg, K., 1987. "The method of moving asymptotes – a new method for structural optimization". *Int. J. Numer. Meth. Engrg.*, **24** [], pp. 359–373.
- [14] Uppala, S., Gao, R., Cowan, S., and Lee, F., 2000. "A biomechanical model of lumbar spine". In Dynamics Systems and Control Division, vol. 1, ASME.
- [15] Rohlmann, A., Neller, S., Claes, L., Bergmann, G., and Wilke, H., 2001. "Influence of a followe load on intradiscal pressure and intersegmental rotation of the lumbar spine". *SPINE*, **26** (24) [], pp. E557–E561.
- [16] Zander, T., Rohlmann, A., Klöckner, C., and Bergmann, G., 2002. "Comparison of the mechanical behavior of the lumbar spine following mono- and bisegmental stabilization". *Clinical Biomechanics* (17) [], pp. 439–445.
- [17] Lewis, G., 1997. "Properties of acrylic bone cement: State of the art review". *CCC 0021-9304* [], pp. 155–182.